International Journal of Engineering Research and Technology. ISSN 0974-3154, Volume 12, Number 8 (2019), pp. 1157-1163

Peak Wind Coefficients of Piloti Cladding on High Rise Buildings

Jang-Youl You[1], Min-Woo Park[2] and Ki-Pyo You[3*]

[1] Songwon University, Department of Architecture Engineering, Gwangju, 61756, Republic of Korea.
[2] Chonbuk University, Department of Architecture Engineering, Jeonju, 54896, Republic of Korea.
[3] Chonbuk University, Department of Architecture Engineering, Jeonju, 54896, Republic of Korea.
** Corresponding author*

Abstract

Various types of pilotis are used in the construction of the lower stories of high rise buildings. The interior finishes of pilotis in downtown buildings may be damaged by strong winds, compromising pedestrian safety. However, the wind pressure coefficients facilitating appropriate cladding of end and corner pilotis (often evident in high rise buildings) are poorly understood. Wind pressure experiments showed that, for end pilotis, the lowest peak wind-pressure coefficients –2.7 were evident at wind angles of 0 and 270ºC, thus parallel to the wind direction. For corner pilotis, the minimum peak wind-pressure coefficient was –2.0 at the center of the ceiling near the wind angle of the building corners.

Keywords: Piloti, Peak Wind Pressure Coefficient, Coner Edge Piloti, End Edge Piloti

I. INTRODUCTION

Recently, downtown outdoor thermal comfort has been compromised by the high temperatures of heat islands. Downtown residents are very sensitive to changes in the outdoor thermal environment [1–5]. Open spaces, building layout and shape, green islands, and water features are used to improve the downtown thermal environment. In a survey of resident thermal comfort, Uchida et al. showed that ponds and green areas improved the thermal environment in summer [6]. Chen et al. performed field measurements to explore the effects of apartment block plans, external changes, and location on the outdoor thermal environment of Shenzhen (China) [7]. Xuan et al. [8] and Yang et al. [9] presented building layouts minimizing the outdoor thermal loads caused by climate change. The cited authors derived optimal D/H ratios, where D is the length of the building and H is the height, and used these data to plan urban ventilation and awning installations in Sendai, Japan and Guangzhou, China. The wind-velocity distributions around buildings were affected by the building length; longer buildings reduced wind velocity, compromising ventilation and thermal comfort. Zeng, Qinli, & Akashi (2014) used computer flow dynamics (CFD) to measure air currents around open and enclosed pilotis in the lower stories of buildings [10]. Piloti "openness" ranged from 0–80%. As openness increased, the average wind velocity also increased. Jo & Gil (2014) used CFD to explore how openness affected wind strength; the more enclosed the piloti, the higher the wind velocity and the larger the extent of negative pressure. Although such an effect would be expected, no prior evaluation of wind-pressure coefficients inside pilotis according to increased wind velocity has appeared [11]. Won (2014) analyzed factors affecting ventilation throughout large apartment buildings and open pilotis [12]. Tower-type layouts exhibited higher wind-velocity ratios than plate/grid-type layouts. Although wind velocity changes within apartment complex pilotis have thus been evaluated, the piloti wind ("openness wind") is a building-related wind [13-15] that acts in concert with downtown air currents to create windblasts as wind flows around the pilotis, frequently damaging the cladding (Fig. 1). Thus, wind-pressure coefficients facilitating accurate cladding design are required. However, there have been few studies on appropriate peak wind-pressure coefficients considering cladding wind-loading. Using a wind tunnel, we developed a peak wind-pressure coefficient that will aid in the design of cladding for the ceilings and walls of end and corner pilotis installed in the lower stories of high-rise buildings.

Fig. 1. Damage to exterior piloti

II. WIND TUNNEL EXPERIMENT

II.I Model

Four experimental models were created to investigate the effects on the wind pressure coefficients on the ceiling and wall in a piloti. The experiment used a 40-story square building with a length (B) and width (D) of 36 m and a height (H) of 120 m. It was a high rise building with a long side to short side ratio of 1

International Journal of Engineering Research and Technology. ISSN 0974-3154, Volume 12, Number 8 (2019), pp. 1157-1163

and a height to width ratio of 3.3. At the lower levels, end pilotis were installed on one side and corner pilotis were installed at a corner. The wind tunnel experiment models were produced by changing piloti height (h) from 4.5 m to 9 m with a fixed length (b) to width (d) ratio of 1:0.33 for end pilotis and 1:1 for corner pilotis. The models were created using acrylic at a scale of 1/300. The dimensions of the models are listed in Tab. 1. Pressure measurement taps were installed on the ceilings and walls of the pilotis to examine the characteristics of the piloti wind pressure distribution. In Case 1, the piloti type was end piloti, height was 4.5 m, and 55 pressure measurement taps (33 on ceiling and 22 on wall) were installed. In Case 2, the piloti type was end piloti, height was 9 m, and 66 pressure measurement taps (33 on ceiling and 33 on wall) were installed. In Case 3, the piloti type was corner piloti, height was 4.5 m, and 45 pressure measurement taps (25 on ceiling and 10 each on two walls) were installed. In Case 4, the piloti type was corner piloti, height was 9 m, and 55 pressure measurement taps (25 on ceiling and 15 each on two walls) were installed. The pressure measurement taps were arranged at equal intervals. Fig. 2 shows the prototype dimensions. Fig. 3 shows the experimental model installed in a wind tunnel.

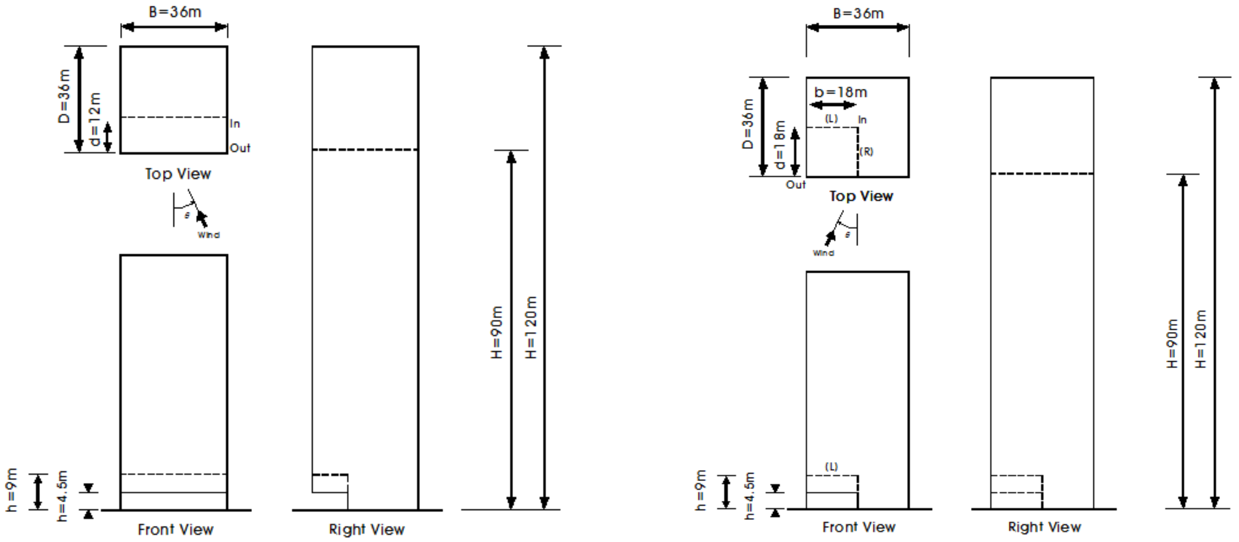

(a) Case 1　　　　(b) Case 2

Fig. 2. Prototype dimensions

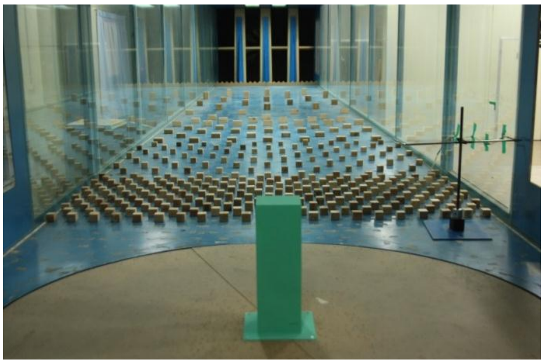

Fig. 3. Experiment model installed within the wind tunnel

II.II Wind Tunnel Experiment

The wind tunnel experiment for the ceilings and walls of pilotis in high rise buildings used an Eiffel-type boundary layer wind tunnel owned by the Boundary Layer Wind Tunnel Laboratory of Chonbuk National University. The dimensions of the wind tunnel measurement unit were 18 m (L) × 2.1 m (W) × 1.7 m (H), and the wind speed range was 0.3 to 12 m/s. For the turbulent boundary layer applied to the experiment, surface roughness classification B (α = 0.22) was used, which corresponds to an urban area with medium to low-rise buildings. The average wind speed by height in the wind tunnel and the vertical distribution of turbulence intensity are shown in Fig. 4. The solid line indicates a theorem by the exponential law, and Tab. 2 shows the similarity law used in the wind tunnel experiment. The air flow in the wind tunnel was measured using a hot wire anemometer (IFA-300).

Table 1. Prototype and model sizes

Classification		Prototype(m)						Model(cm)					
		B	D	H	Piloti			B	D	H	Piloti		
					b	d	h				b	d	h
End Piloti	CASE1	36	36	120	36	12	4.5	12	12	40	12	3	1.5
	CASE2						9						3
Corner Piloti	CASE3	36	36	120	18	18	4.5	12	12	40	6	6	1.5
	CASE4						9						3

The experimental wind speed was 5 m/s. The experimental angles were varied from 0° to 350° in 10° intervals in 36 directions. Fig. 5 shows the experimental wind angles. A 120-cm long tube was used for wind pressure measurement in the experiment. Wind pressure signals were calibrated using a restrictor at a specific position of the tube. Each wind pressure measured in the experiment is indicated as a dimensionless quantity. The maximum/minimum peak wind pressure coefficients are defined by Eq. 1 and 2, respectively.

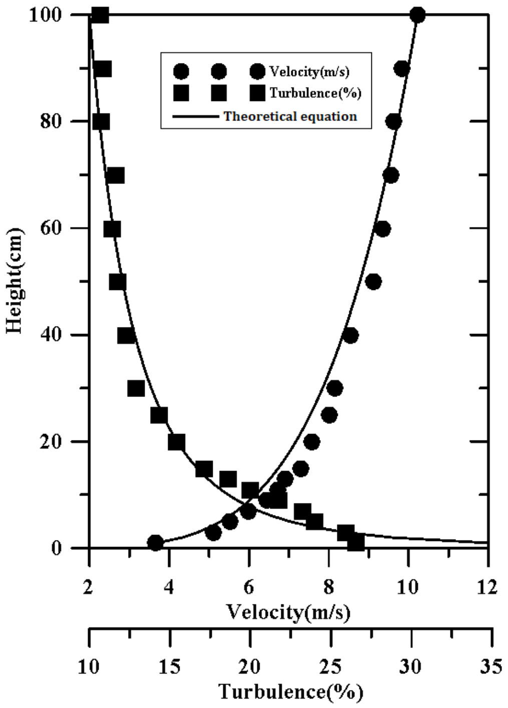

Fig. 4. Vertical distribution of average wind speed and turbulence intensity

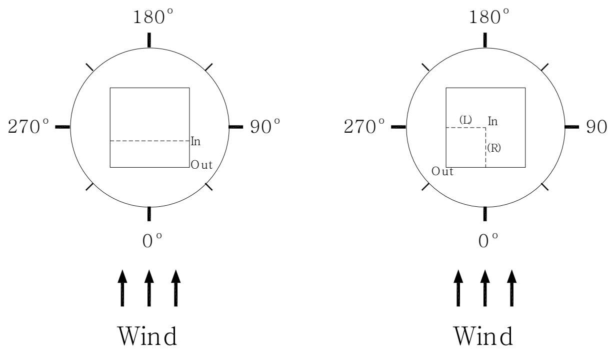

(a) End Piloti (b) Conner Piloti

Fig. 5. Experimental wind angles

Table 2. Similarity law

Velocity scale	1/8.1	Basic wind velocity	Experiment velocity
		40.6m/s	5m/s
Model scale	1/300		
Time scale	1/36.9		
Ensemble average	10 times		
Moving average time	1 sec		
Sampling Frequency	200 Hz		
Wind direction	36 Direction(0° to 350°, 10° interval)		
Roughness division	Roughness B		

Maximum peak wind pressure coefficient:

$$C_{pmax} = P_{max}/q_h \quad (1)$$

Minimum peak wind pressure coefficient:

$$C_{pmin} = P_{min}/q_h \quad (2)$$

III. EXPERIMENTAL RESULTS

The experimental results were analyzed based on the maximum/minimum peak wind pressure coefficients used in the wind load design for the exterior materials in the end and corner pilotis. First, the distribution of the maximum/ minimum peak wind pressure coefficients was determined for all wind angles. Second, the distribution of the maximum / minimum peak wind pressure coefficients was analyzed according to changing wind angles.

III.I Distribution Characteristics of Maximum/Minimum Peak Wind Pressure Coefficients for All Wind Angles

III.I.I End Pilotis

Figs. 6 and 7 show the distributions of the maximum / minimum peak wind pressure coefficients on the ceiling and walls according of a piloti installed at the side of high rise building according to change in height. The maximum peak wind pressure coefficient is 0.9–1.6 on the ceiling and 1.0–1.65 on the walls. The maximum peak wind pressure coefficients on the ceiling and walls at the center are higher than those at both sides. The minimum peak wind pressure coefficient is -1.75–-2.75 on the ceiling and -1.75–-2.35 on the walls. The minimum peak wind pressure coefficient on the ceiling increases from the center toward both sides (based on absolute values). When piloti height increases from 4.5 m to 9 m, the maximum peak wind pressure coefficient decreases from 1.6 to 1.35 and the minimum peak wind pressure coefficient decreases from -2.75 to -2.25 (based on absolute values). It appears that small vortices appear inside the piloti when piloti height decreases.

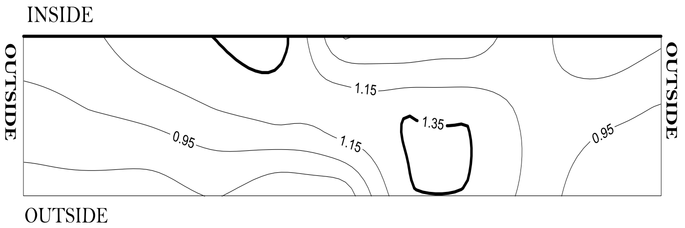

(a) maximum peak pressure coefficient of ceiling (h=4.5m)

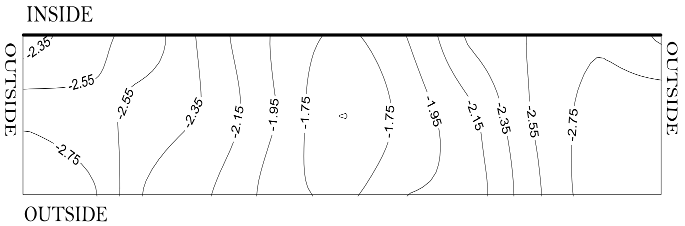

(b) minimum peak pressure coefficient of ceiling (h=4.5m)

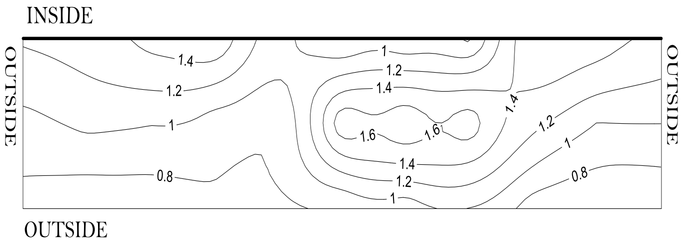

(c) maximum peak pressure coefficient of ceiling (h=9.0m)

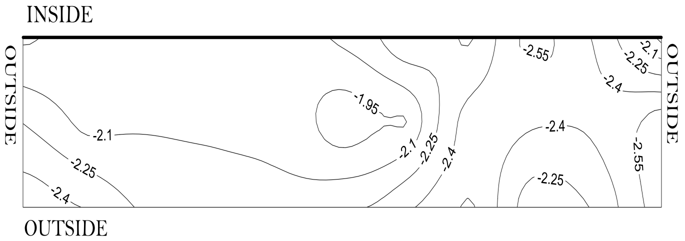

(d) maximum peak pressure coefficient of ceiling (h=9.0m)

Fig. 6. Distribution of peak wind pressure coefficients on the ceiling of end piloti according to change in height

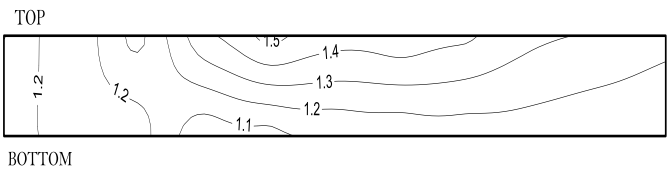

(a) maximum peak pressure coefficient of wall (h=4.5m)

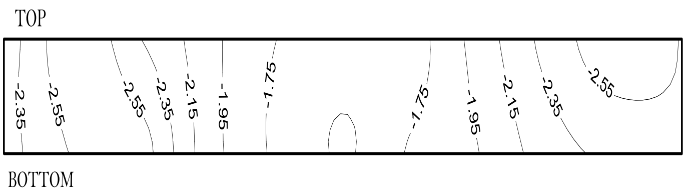

(b) minimum peak pressure coefficient of wall (h=4.5m)

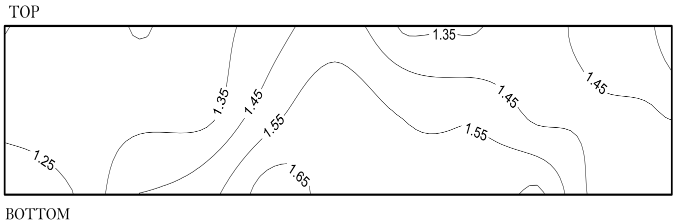

(c) maximum peak pressure coefficient of wall (h=9.0m)

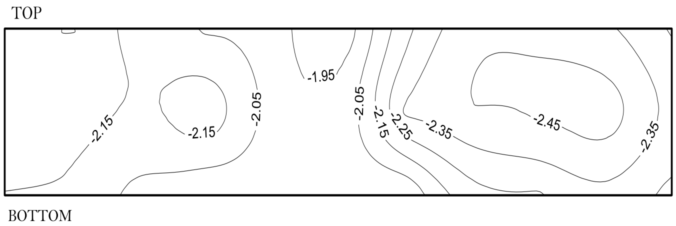

(d) minimum peak pressure coefficient of wall (h=9.0m)

Fig. 7. Distribution of peak wind pressure coefficients on the walls of end piloti according to change in height

III.I.II Corner Pilotis

Figs. 8 and 9 show the distributions of the maximum/minimum peak wind pressure coefficients according to the change in the height of a piloti installed at a corner of a high rise building. The maximum peak wind pressure coefficient is 0.95–1.5 on the ceiling and 1.2–1.5 on the walls. The maximum peak wind pressure coefficient increases from the outside to the inside of the ceiling. The highest maximum peak wind pressure coefficient is at the inner corner. The minimum peak wind pressure coefficient is -1.7–-2.0 on the ceiling and -1.6–-1.86 on the walls. The highest values (based on absolute values) of the minimum peak wind pressure coefficient are distributed along concentric circles in the diagonal direction from the corner of the ceiling. The strong external pressure appears to be the effect of the swirl vortex inside the piloti. The highest values of the minimum peak wind pressure coefficients (based on absolute values) are distributed at all corners on the ceiling. When piloti height increases from 4.5 m to 9 m, the maximum peak wind pressure coefficient increases from 1.35 to 1.45, and the minimum peak wind pressure coefficient increases from -1.95 to -2.0 (based on absolute values).

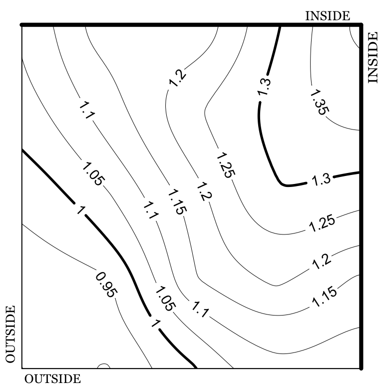

(a) maximum peak pressure coefficient of ceiling (h=4.5m)

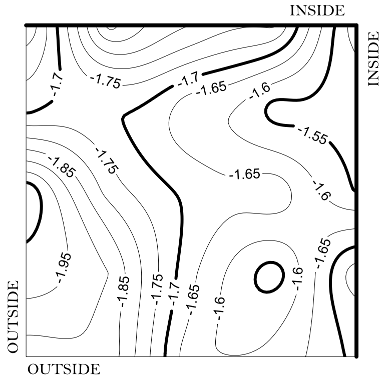

(b) minimum peak pressure coefficient of ceiling (h=4.5m)

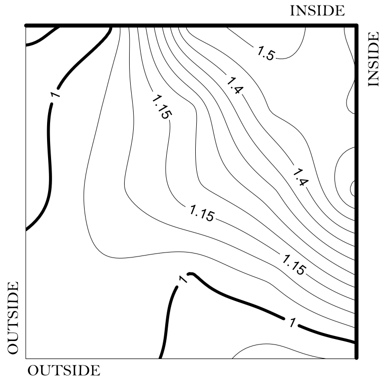

(c) maximum peak pressure coefficient of ceiling (h=9.0m)

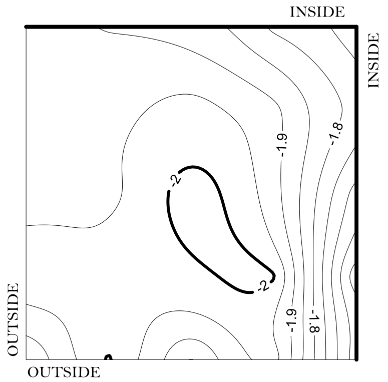

(d) maximum peak pressure coefficient of ceiling (h=9.0m)

Fig. 8. Distribution of peak wind pressure coefficients on the ceiling based on change in the height of the corner piloti

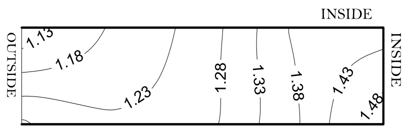

(a-1) maximum peak pressure coefficient of left wall (h=4.5m)

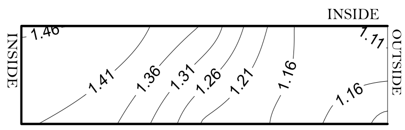

(a-2) maximum peak pressure coefficient of right wall (h=4.5m)

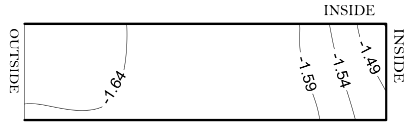

(a-3) minimum peak pressure coefficient of left wall (h=4.5m)

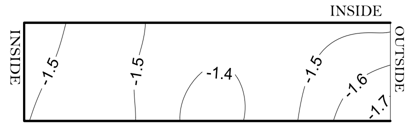

(a-4) minimum peak pressure coefficient of right wall (h=4.5m)

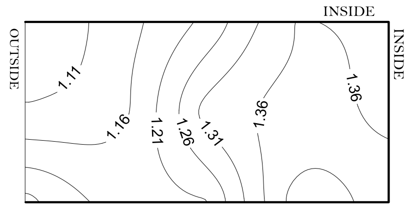

(b-1) maximum peak pressure coefficient of left wall (h=9m)

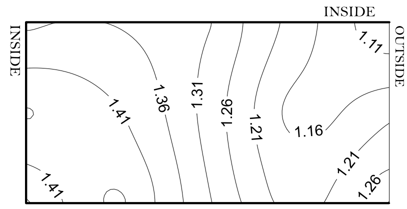

(b-2) maximum peak pressure coefficient of right wall (h=9m)

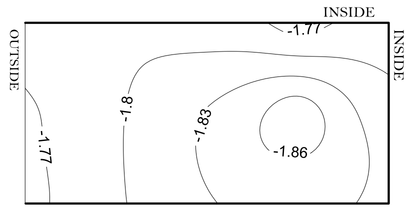

(b-3) minimum peak pressure coefficient of left wall (h=9m)

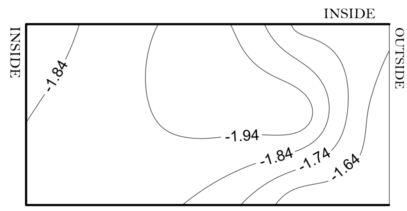

(b-4) minimum peak pressure coefficient of right wall(h=9m)

Fig. 9. Distribution of peak wind pressure coefficients on the walls based on change in the height of the corner piloti

III.II Peak wind pressure coefficient based on change in wind angle

The distribution characteristics of the peak wind pressure coefficients were analyzed based on the change in wind angle. Fig. 10 shows the distributions of the maximum/minimum peak wind pressure coefficients for 36 wind angles for the end and corner pilotis. The end piloti shows the maximum peak wind pressure coefficient at wind angles of 0° and 350° when the piloti axis is along the wind direction and the minimum peak wind pressure coefficient at wind angles of 90° and 270° when the axis is perpendicular to the wind. The corner piloti shows the highest maximum/minimum peak wind pressure coefficients at the wind angles of 270° and 0°.

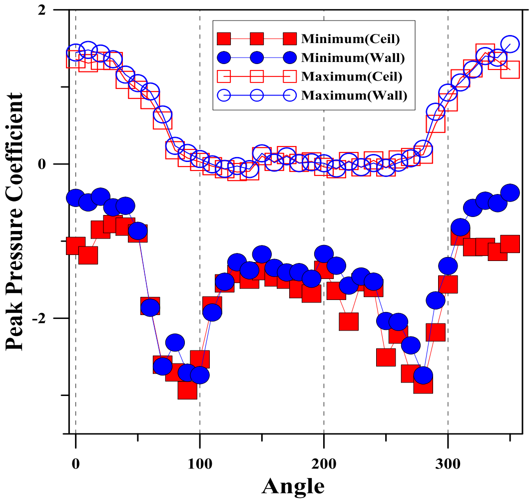

(a) End piloti (h=4.5m)

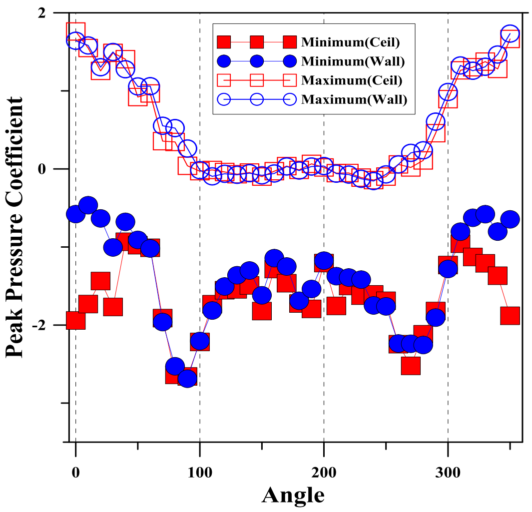

(b) End piloti (h=9.0m)

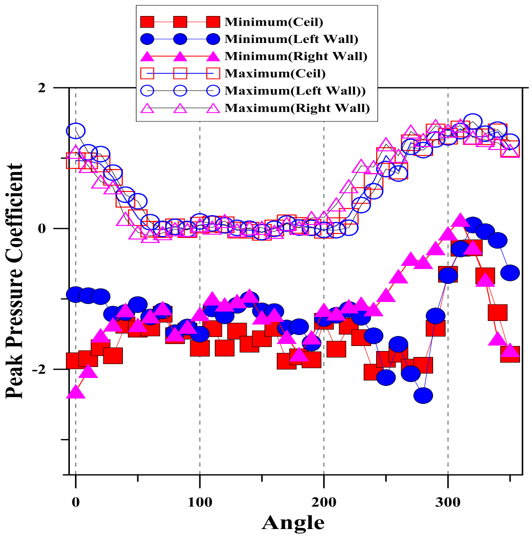

(c) Corner piloti (h=4.5m)

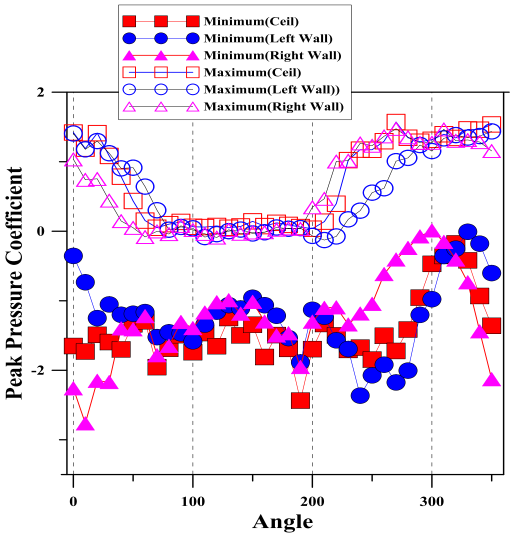

(d) Corner piloti (h=9.0m)

Fig. 10. Distributions of maximum/minimum peak wind pressure coefficient based on change in wind angle

Fig. 11 shows the distributions of the maximum/minimum peak wind pressure coefficients on the ceiling and walls of end piloti at wind angles of 0° and 270°. The maximum peak wind pressure coefficient of the end piloti appears at 0°. The maximum peak wind pressure coefficients on the ceiling and walls all appear at the center. The position changes according to wall height. When piloti height is 4.5 m, the coefficient is 1.36 at the bottom of the wall and close to the ceiling. On the ceiling, the highest maximum peak wind pressure coefficient appears at the center of the corner that is in contact with the wall. However, when piloti height is 9 m, the maximum peak wind pressure coefficient is larger by approximately 19% and forms a large circular shape at the center. The minimum peak wind pressure coefficient decreases from the end corner in the direction opposite to the wind. The minimum peak wind pressure coefficient at the end corner decreases as piloti height increases. However, the minimum values are distributed broadly toward the center.

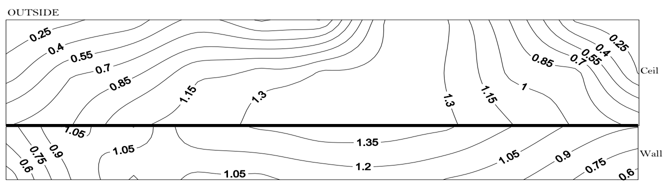

(a) maximum peak pressure coefficient
(h=4.5m, wind direction 0°)

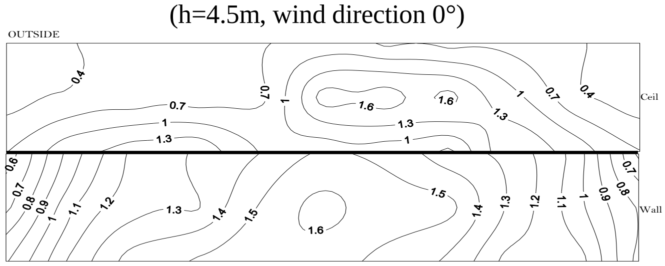

(b) maximum peak pressure coefficient
(h=9.0m, wind direction 0°)

International Journal of Engineering Research and Technology. ISSN 0974-3154, Volume 12, Number 8 (2019), pp. 1157-1163

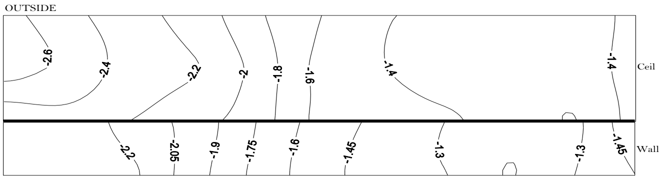

(c) minimum peak pressure coefficient
(h=4.5m, wind direction 270°)

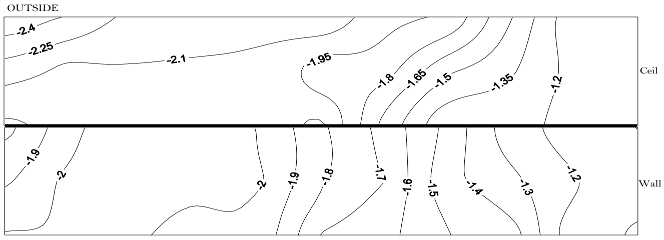

(d) minimum peak pressure coefficient
(h=9.0m, wind direction 270°)

Fig. 11. Distributions of maximum/minimum peak wind pressure coefficient on the ceiling and walls of end piloti (wind angle = 0°, 270°)

Fig. 12 shows the distributions of the maximum/minimum peak wind pressure coefficients on the ceiling and walls of a corner piloti at the wind angles of 270° and 320°. The maximum peak wind pressure coefficient is 1.0–1.4 on the ceiling and 1.1–1.4 on the walls. The wind pressure coefficient increases toward the inner corner on the piloti ceiling and walls. When piloti height increases, a larger wind pressure coefficient is measured in the direction of the wind. The minimum peak wind pressure coefficient is higher than the lowest value of -1.8 on the piloti axis along the wind direction. Furthermore, the minimum peak wind pressure coefficient is distributed in concentric shapes on the wall. The concentric shapes are observed more clearly as piloti height increases.

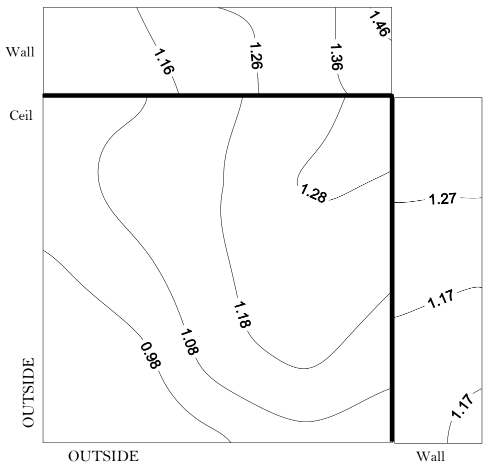

(a) maximum (h=4.5m, wind direction 320°)

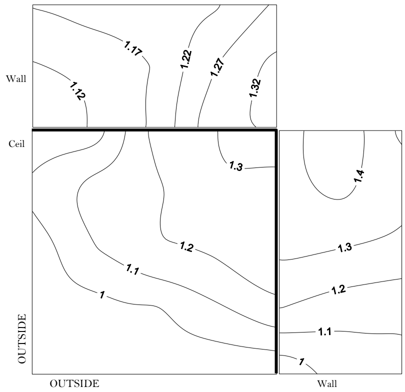

(b) maximum (h=9.0m, wind direction 320°)

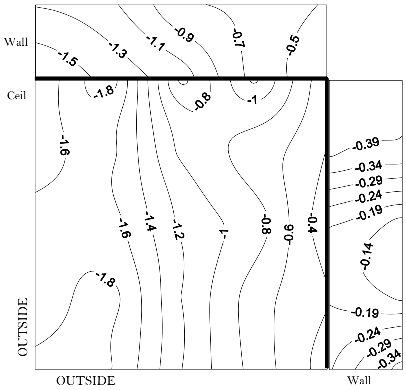

(c) minimum (h=4.5m, wind direction 270°)

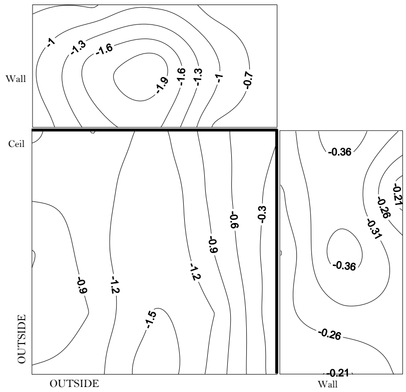

(d) minimum (h=9.0m, wind direction 270°)

Fig. 12. Distributions of maximum/minimum peak wind pressure coefficient on the ceiling and walls of corner piloti (wind angle = 270°, 320°)

IV. CONCLUSION

1) For the end piloti, the maximum peak wind pressure coefficient is larger at the center of the ceiling and the minimum peak wind pressure coefficient is larger at the left and right corners exposed to the outside of the ceiling. The peak wind pressure coefficient decreases as piloti height increases. The peak wind pressure coefficient on the ceiling is larger than that on the walls for the corner piloti. On the ceiling, the maximum peak wind pressure coefficient is larger at the corner and the minimum peak wind pressure coefficient is larger at the center of the ceiling. The peak wind pressure coefficient increases with piloti height owing to the vortex inside the piloti.

2) For end piloti, the peak wind pressure coefficients, in terms of wind-angle changes, were –2.4 for the ceilings and –2.7 for the walls at wind angles of 90° and 270°. For corner piloti, the figures were –2.04 for ceilings and –2.4 for walls. The peak wind pressure coefficients facilitating cladding design were obtained at specific angles. When designing pilotis for high rise buildings, our coefficients can be used to locate piloti by reference to the principal wind angle of the building site, and to design safe piloti finishes resisting both building related and strong external winds.

ACKNOWLEDGMENTS

This study was supported by research fund from Songwon University.

REFERENCES

[1] Amindeldar S, Heidari S, Khalili M. The effect of personal and microclimatic variables on outdoor thermal comfort: A field study in Tehran in cold season, Sustainable Cities and Society. 2017:32:153–159.

[2] Chatzidimitriou A, Yannas S. Street canyon design and improvement potential for urban open spaces; the influence of canyon aspect ratio and orientation on microclimate and outdoor comfort, Sustainable Cities and Society. 2017:33: 85–101.

[3] Li Y, Huang G, Wu H, Xu T. Feasibility study of a PCM storage tank integrated heating system for outdoor swimming pools during the winter season, Applied Thermal Engineering. 2018:134:490–500.

[4] Bonggeun S, Kyunghun P. Contribution of Greening and High-Albedo Coatings to Improvements in the Thermal Environment in Complex Urban Areas, Advances in Meteorology. 2015:14. article 792172.

[5] Kubota T, Miura M, Tominaga Y, Mochida A. Wind tunnel tests on the relationship between building density and pedestrian-level wind velocity: Development of guidelines for realizing acceptable wind environment in residential neighborhoods, Building and Environment. 2008:43:1699–1708.

[6] Uchida M, Mochida A, Sasaki K, Tonouchi T. Field measurements on turbulent flowfield and thermal environment in and around biotope with pond and green space, The seventh International Conference on Urban Climate, Yokohama, Japan . 2009.

[7] Chen H, Ooka R, Harayama K, Kato S, Li X, Study on outdoor thermal environment of apartment block in Shenzhen, China with coupled simulation of convection, radiation and conduction, Energy and Buildings. 2004: 36: 1247–58.

[8] Xuan Y, Li Q, Yang G, Mochida A. Fundamental Study on Building Arrangement to Maximize Thermal Acceptability of Outdoors at Different Latitudes Part 1: The Characteristics of Wind Velocity Distributions in Different Building Arrangements in Guangzhou and Sendai, Technical papers of annual meeting of Architectural Institute of Japan. 2013: 873-874.

[9] Yang G, Li Q, Xuan Y, Mochida A. Fundamental Study on Building Arrangement to Maximize Thermal Acceptability of Outdoors at Different Latitudes Part 2: The Change of Outdoor Thermal Environment in Different Building Arrangements in Guangzhou and Sendai, Technical papers of annual meeting of Architectural Institute of Japan. 2013: 873-874.

[10] Zeng Z, Qinli D, Akashi M. Effect of piloti on wind environment in residential area in a hot and humid city, Journal of the Wind Engineering Institute of Japan. 2014: 73-78.

[11] Jo J, Gil Y. Evaluation of Wind Effect for Piloti Space of Buildings using Numerical Analysis Method, The Wind Engineering Institute of Korea. 2014:47-50.

[12] Hyung W.G, Kim Y.M, You K.P. Analysis of Change in the Wind Speed Ratio according to Apartment Layout and Solutions, The Scientific World Journal. 2014:9, article 760713.

[13] Zhang X, Tse K.T, Weerasuriya A.U, Li S.W, Kwok K.C.S, Mak C.M, Niu J, Lin Z. Evaluation of pedestrian wind comfort near 'lift-up' buildings with different aspect ratios and central core modifications, Building and Environment. 2017:124: 245–257.

[14] Wu H,Kriksic F. Designing for pedestrian comfort in response to local climate, Journal of Wind Engineering and Industrial Aerodynamics. 2012:104–106:397–407.

[15] Blocken B, Janssen W.D, Van Hooff T. CFD simulation for pedestrian wind comfort and wind safety in urban areas: general decision framework and case study for the Eindhoven University campus, Environment Modelling & Software. 2012:30:15–34